Proceedings of the XVII ECSMGE-2019
Geotechnical Engineering foundation of the future
ISBN 978-9935-9436-1-3

doi: 10.32075/17ECSMGE-2019-0218

Investigation of the bearing behaviour of slender driven piles in clay – Comparison of different static and dynamic methods of pile testing

Etude du comportement au roulement de pieux minces enfoncés dans l'argile - Comparaison des différentes méthodes statiques et dynamiques d'essais de pieux

J. Berndt, O. Reul,
University of Kassel, Germany

B. Schrötter,
TRM Tiroler Rohre GmbH, Hall in Tirol, Austria

M. Hayden,
Keller Grundbau GmbH, Vienna, Austria

ABSTRACT: As part of a joint research project, pile load tests applying various static and dynamic testing methods were performed on slender driven piles, i.e. prefabricated driven cast-iron piles (ductile piles). The tests, carried out in clayey soil at a test site in Austria, comprised conventional static compression and static tension load tests, bi-directional load tests with the Pile HAY-Proof-System® and dynamic load tests using the CAPWAP approach. In the scope of this paper the results of the pile load tests are presented and the bearing behaviour of slender driven piles in clay is discussed in the light of the various testing methods applied.

RÉSUMÉ: Dans le cadre d'un projet de recherche conjoint, des essais de charge de pieux ont été effectués sur des pieux minces enfoncés à l'aide de diverses méthodes d'essais statiques et dynamiques. Les essais, effectués dans un sol argileux sur un site d'essai en Autriche, comprenaient des essais conventionnels de compression statique et de charge de traction statique, des essais de charge bidirectionnelle avec le système Pile HAY-Proof-System® et des essais de charge dynamique selon l'approche CAPWAP. Dans le cadre de ce document, les résultats des essais de charge des pieux sont présentés et le comportement de portance des pieux minces enfoncés dans l'argile est discuté à la lumière des différentes méthodes d'essai appliquées.

Keywords: in-situ pile tests, displacement piles, clay

1 INTRODUCTION

In the German guideline "Recommendations on Piling (EA Pfähle)" by the DGGT (2014) an empirical database for the capacity, i.e. shaft friction $q_{s,k}$ and base resistance $q_{b,k}$, is documented for various pile systems. However, for prefabricated driven cast-iron piles (in the remainder of this paper simply referred to as ductile piles) such a database is not available in the above mentioned EA Pfähle, so far.

To establish a database for ductile piles the collection and evaluation of available pile load tests is currently on its way. As part of this process, pile load tests applying various static and dynamic testing methods were performed on ductile piles at a test site in Austria within a joint research project.

2 PILE SYSTEM

Ductile piles manufactured by TRM Tiroler Rohre GmbH, Austria, consist of ductile, spun cast-iron pipe segments driven in the ground with a hydraulic hammer whereby the surrounding soil is fully displaced. The 5 m long pipe segments are connected by means of spigots and sockets allowing to assemble the required pile length during driving. The first pipe segment is placed in the so called driving shoe which has the same diameter as the pipe in case of a pile without shaft grouting and a larger diameter in case of a pile with shaft grouting (Figure 1).

Piles without shaft grouting are end-bearing piles which require a firm soil layer at pile base level. For piles with shaft grouting, during driving fine grained concrete or cement grout (in the remainder of this paper simply referred to as grout) is permanently pumped through the inside of the pipe. The grout fills the annulus formed by the oversized driving shoe from the pile base to the pile head. Provided the soil surrounding the grouted shaft shows a sufficient strength, piles with shaft grouting are able to transfer a significant share of the load to the soil by mobilizing shaft friction.

Up to now, the socket-spigot system is not designed to transmit tension forces. However, current developments of TRM Tiroler Rohre GmbH aim to optimize the circular socket shape to allow the transmission of tension loads without having to place a tension bar inside the grout filled pipe.

For TRM ductile piles the German general technical approval Z.34.25-230 (DIBt 2017) considers different pipe diameters, namely D_{pipe} = 98 mm, D_{pipe} = 118 mm and D_{pipe} = 170 mm as well as a pipe thickness between S = 6 mm to S = 13 mm. The diameter of the driving shoe must be large enough to provide a grout cover in the area of the sockets of at least 20 mm. Depending on pipe diameter D_{pipe}, pipe thickness S and grout quality (C20/25 or C25/30) the design value of the internal (structural) compression capacity varies between $R_{i,d}$ = 450 kN (D_{pipe} = 98 mm; S = 6 mm; no shaft grouting) and $R_{i,d}$ = 2137 kN (D_{pipe} = 170 mm; S = 13 mm; with shaft grouting) according to Z.34.25-230 (DIBt 2017). Although the thickness of grout cover at the pile shaft is not considered in the calculation of the structural capacity, for piles without shaft grouting a reduced outer diameter is taken into account because of rusting.

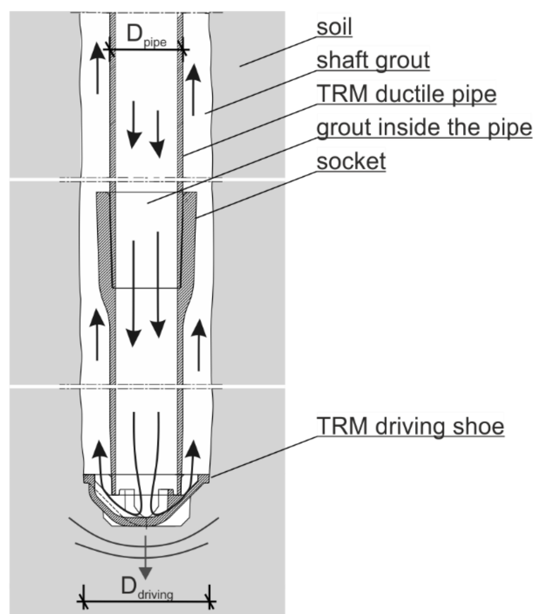

Figure 1. TRM ductile pile wih shaft grouting

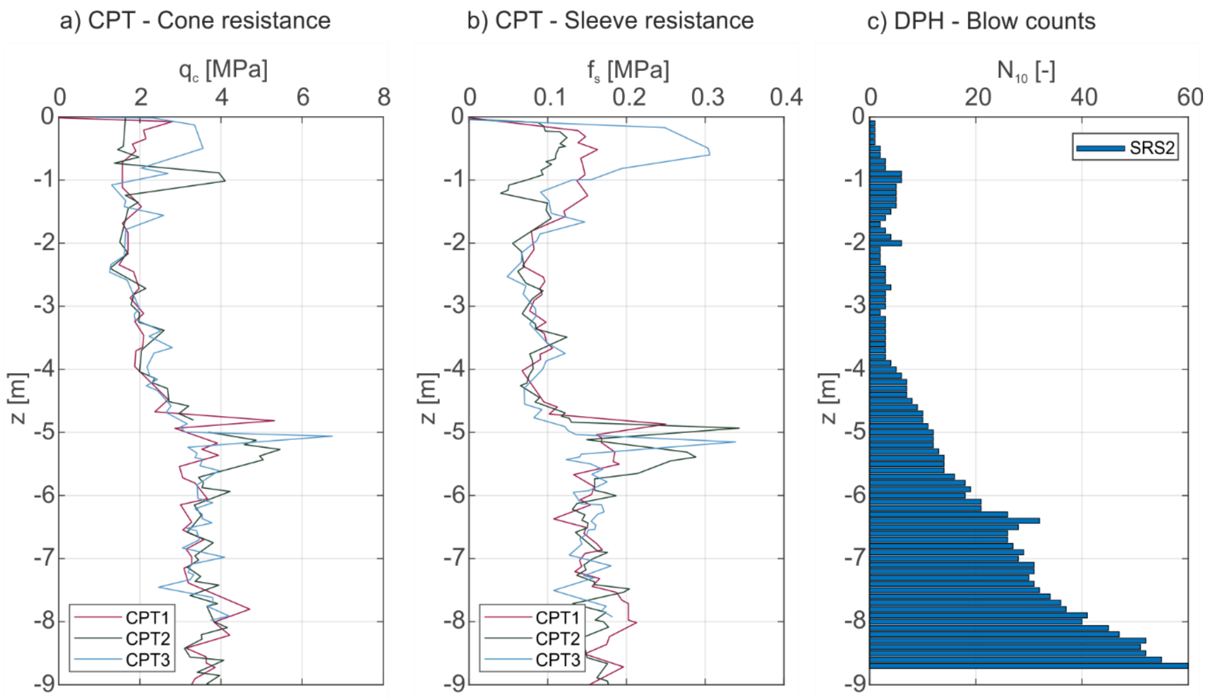

Figure 2. Site investigation by means of CPT- and DPH-soundings

3 TEST PROGRAMME

3.1 Ground conditions at the test site

The test site is located in vicinity to a number of wind turbines at Hollern, about 50 km east of Vienna. In a maximum distance of 30 m core drillings, cone penetration tests (CPT) and heavy dynamic probing (DPH) was carried out, partially for the site investigation of the above mentioned wind turbines. The results of CPT- and DPH-soundings (Figure 2) show fairly uniform soil conditions across the site. In the scope of the site investigations for the wind turbine the soil profile was described as comprising mainly of slightly sandy clays and silts with the stiffness increasing significantly with depth (Table 1).

Small amounts of stratum water was found in the boreholes. However, the groundwater level is situated more than 15 m below ground surface and doesn't affect the pile load tests.

Table 1. Soil profile at the test site

Depth [m]	**Description**
0.5 – 3.5	plastic to high plastic, slightly sandy clay; soft to firm consistency; thin layers (<30 cm) of sand
3.5 – 6.0	plastic to high plastic, slightly sandy clay and silt; firm to stiff consistency; thin layers of sand
6.0 - >>	plastic to high plastic, slightly sandy clay and silt; stiff to very stiff consistency

3.2 Test piles

At the test site a total of twelve pile load tests on shaft grouted TRM ductile piles (L_{pile} = 9,0 m; D_{pipe} = 118 mm; S = 7.5 mm to 9.0 mm; $D_{driving}$ = 220 mm) were carried out. The pile load tests varied the test methods, the time between installation and testing, geometry and material of the driving shoe, the shape of the pipe socket and the pipe segment length.

The prototype trilobular-shaped socket, which is still in its early development phase, allows the application of tension loads without the requirement to place a tension bar inside the grout filled pipe.

Table 2 summarizes the various test pile (PP) configurations. Figure 3 shows the layout of the test piles in the ground plan.

Table 2. Test piles

Pile	Test method	Time [d]	Driving shoe		Socket shape	Segment length [m]	Strain measurement	
			Shape	Material			Strain gauges	Fibre optics
PP3a	static, compression	7	conical	cast-iron	circular	5.0/4.0	+	+
PP3b	static, compression	28	conical	cast-iron	circular	5.0/4.0	-	-
PP7a	static, tension	7	conical	cast-iron	trilobular	5.0/4.0	-	+
PP8a	static, tension	7	conical	cast-iron	trilobular	2.5/5.0/1.5	-	-
PP2a	static, Pile H-P-S	7	conical	steel	circular	5.0/4.0	-	-
PP2b	static, Pile H-P-S	28	conical	steel	circular	5.0/4.0	-	-
PP5a	static, Pile H-P-S	7	flat	steel	circular	5.0/4.0	-	-
PP6a	static, Pile H-P-S	7	conical	cast-iron	circular	5.0/4.0	-	-
PP1a	dynamic, high-strain	7	conical	cast-iron	circular	5.0/4.0	-	-
PP1b	dynamic, high-strain	28	conical	cast-iron	circular	5.0/4.0	-	-
PP4a	dynamic, high-strain	7	conical	cast-iron	circular	5.0/4.0	-	-
PP4b	dynamic, high-strain	28	conical	cast-iron	circular	5.0/4.0	-	-

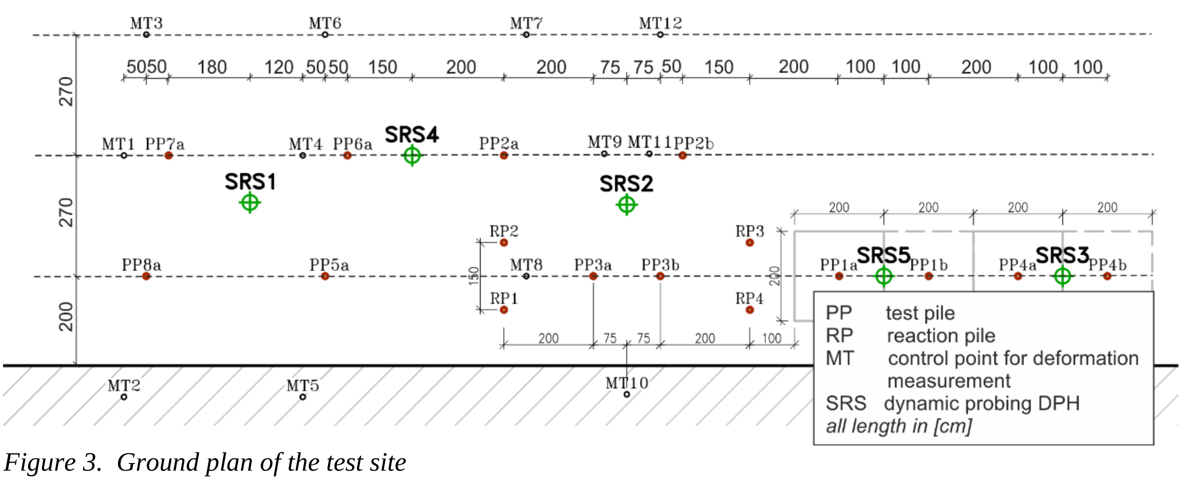

Figure 3. Ground plan of the test site

3.3 Test methods

3.3.1 Conventional static load tests

Four conventional static load tests were carried out, namely two compression tests (PP3a, PP3b) and two tension tests (PP7a, PP8a). The compression load tests required the installation of four reaction piles (RP) with pile length of $L_p = 10$ m. In all tests the load applied at the pile head and the pile head displacements were measured. For two tests additionally strain measurements by means of strain gauges (PP3a) and fibre optic measurements (PP3a, PP7a) were carried out. The presentation of the strain measurements is beyond the scope of this paper, though.

The fibre optic measurements were carried out by Institute of Engineering Geodesy and Measurement Systems, Graz University of Technology, Austria.

3.3.2 Bi-directional static load tests – Pile HAY-Proof-System® (Pile H-P-S)

In addition to the conventional static compression and tension load tests, four bi-directional static pile load tests according to the Pile HAY-Proof-System® (Pile H-P-S) were carried out. Pile H-P-S tests allow for the separate measurement of shaft and base resistance. Figure 4 shows the schematic sketch of the static system on which the Pile H-P-S is based. Since the pile base acts as the abutment for the pile shaft and vice versa, no reaction piles are required. In a load test according to the Pile-H-P-S the following failure modes can occur:

1. Ultimate shaft resistance R_s is reached first.
2. Ultimate base resistance R_b is reached first.
3. Shaft resistance and base resistance are reached simultaneously.
4. Internal capacity is reached (structural failue).

For failure mode No. 2 a conventional tension load test will be carried out subsequently to establish the ultimate shaft resistance.

The load and displacement measurements of the static load tests were carried out by geo-proof, Austria.

3.3.3 Dynamic load tests – High strain tests

Dynamic load tests were carried out on the test piles PP1a, PP1b, PP4a and PP4b. The load for the high strain tests was applied by means of a loading system with a free fall mass of m_{FG} = 5000 kg and drop heights between h = 15 cm and h = 57 cm.

The measurements of the dynamic tests and the evaluation of the data by means of the CAPWAP method were carried out by GSP mbH, Germany.

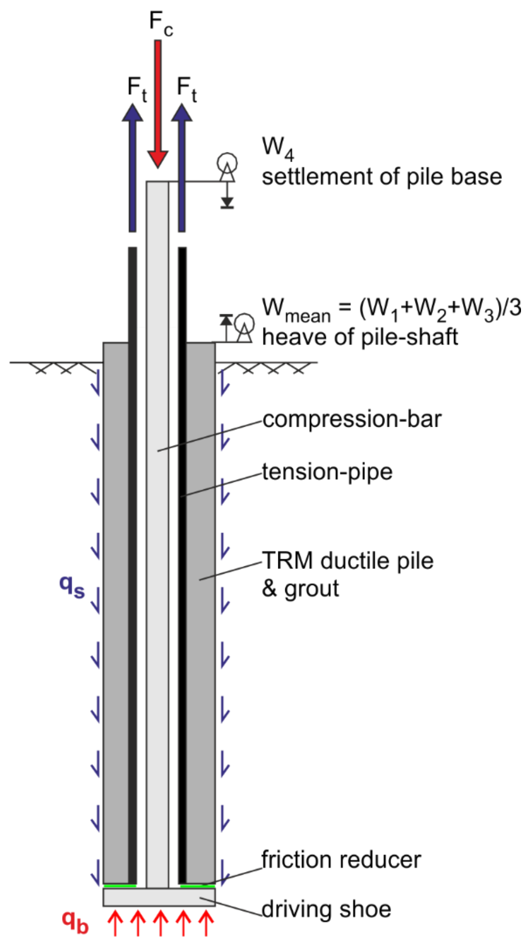

Figure 4. Schematic sketch of the Pile HAY-Proof-System®

4 RESULTS

4.1 Ultimate bearing capacity

4.1.1 General remarks

The results of the pile load tests in terms of the ultimate bearing capacity are summarized in Table 3 where

- the pile diameter D_{pile} is back-calculated from the grout volume recorded for the specific pile,
- the shaft friction $q_{s,m}$ is derived from the shaft resitance $R_{s,m}$ applying D_{pile},
- the unit base resistance $q_{b,m}$ is derived from the base resistance $R_{b,m}$ applying the nomimal diameter of the driving shoe $D_{driving}$ = 220 mm.

4.1.2 Static load tests

All piles in the Pile H-P-S tests showed the same failure mode with the ultimate base resistance R_b reached before the ultimate shaft resistance R_s. The shaft resistance was then established carrying out a conventional static tension test, i.e. by applying a tension force on the pile by means of a reaction beam.

In the conventional static compression tests and the Pile H-P-S tests the range of resistances was measured between R_m = 600 kN (PP3b) and R_m = 885 kN (PP6a). The shaft resistances measured in conventional static tension tests and the Pile H-P-S test lies in a bandwidth between $R_{s,m}$ = 500 kN (PP5a) and $R_{s,m}$ =796 kN (PP6a). However, since structural failure occurred for tension pile PP8a the values documented in Table 3 don’t represent the ultimate bearing capacity of this pile.

With the shaft friction in a range between $q_{s,m}$ = 76 kN/m² (PP5a) and $q_{s,m}$ =110 kN/m² (PP6a) the conventional static load tests and the Pile H-P-S tests are in reasonable agreement. For three out of the four piles where the unit base resistance could be established by means of the Pile H-P-S tests the bandwidth of results was $q_{b,m}$ = 1578 kN/m² (PP2b) to $q_{b,m}$ = 2341 kN/m² (PP6a). The test on pile PP5a with the flat driving shoe showed a significinatly higher unit base resistance of $q_{s,m}$ =7892 kN/m² but also the smallest value for the shaft friction.

A set-up, i.e. an increase of pile capacity with time, could not be observed in the static load tests. On the contrary, the resistances decreased between R_m = 800 kN (PP3a; 7 d) and R_m = 600 kN (PP3b; 28 d) and between R_m = 781 kN (PP2a; 7 d) and R_m = 710 kN (PP2b; 28 d), respectively. However, it has to be noted that the tests after 28 d have been carried out for different piles than the tests after 7 d leaving it open to discussion wether differences in the soil conditions and/or pile geomtry are the causes for this somewhat unexpected result.

4.1.3 Dynamic load tests

The dynamic pile load tests showed significantly higher resistances R_m than the static load test. While the shaft resistances measured with values between $R_{s,m}$ = 651 kN (PP1a) and $R_{s,m}$ = 807 kN (PP4b) lie in the same range as for the static tests, the base resistance with values between $R_{b,m}$ = 489 kN (PP1a) and $R_{b,m}$ = 654 kN (PP1b) is higher by a factor of 7 (in average) than measured in the static tests (leaving pile PP5a with the flat driving shoe beside).

The phenomena of resistances derived from dynamic tests being significantly higher than resistances gained from static tests, especially in clayey soils is well known for different pile systems (e. g. Briaud et al. 2000; Klingmüller & Schallert 2012; Svinkin 2011, Wehr et al. 2015). Fleming et al. (2009) point out that the dynamic base capacity may exceed the static capacity significantly due to viscous effects with the differences more pronounced in soft cohesive soils.

In opposition to the static tests, the dynamic tests also show a set-up with the pile resistances increasing between R_m = 1140 kN (PP1a; 7 d) and R_m = 1196 kN (PP4a; 7 d) to R_m = 1451 kN (PP1b; 28 d) and R_m = 1425 kN (PP4b; 28 d), respectively.

Table 3. Results – ultimate load-bearing capacity

Pile	Test method	Time [d]	Driving shoe	D_{pile} [m]	$R_{b,m}$ [kN]	$q_{b,m}$ [kN/m²]	$R_{s,m}$ [kN]	$q_{s,m}$ [kN/m²]	R_m [kN]
PP3a	static, compression	7	conical, cast-iron	0.24	-	-	-	-	800
PP3b	static, compression	28	conical, cast-iron	0.23	-	-	-	-	600
PP7a	static, tension	7	conical, cast-iron	0.24	-	-	598	89	598
PP8a	static, tension	7	conical, cast-iron	0.25	-	-	*(596)*	*(85)*	*(596)*
PP2a	static, Pile H-P-S	7	conical, steel	0.23	84	2210	650	101	734
PP2b	static, Pile H-P-S	28	conical, steel	0.24	60	1578	650	97	710
PP5a	static, Pile H-P-S	7	flat, steel	0.23	300	7892	500	76	800
PP6a	static, Pile H-P-S	7	conical, cast-iron	0.26	89	2341	796	110	885
PP1a	dynamic, high-strain	7	conical, cast-iron	0.22	489	12864	651	104	1140
PP1b	dynamic, high-strain	28	conical, cast-iron	0.24	654	17205	797	120	1451
PP4a	dynamic, high-strain	7	conical, cast-iron	0.22	501	13180	695	111	1196
PP4b	dynamic, high-strain	28	conical, cast-iron	0.24	619	16284	807	121	1425

4.1.4 Excavation of piles after the test

All piles were excavated down to a depth between 2 m and 3 m (PP6a: 4 m) below ground level after the test to inspect the shaft grout. Generally, the piles showed a proper shaft grout down to the excavation level. However, for all piles tested dynamically a loss of contact between the ductile pipe and the shaft grout was visible leading to the grout actually break away from the pipe after the excavation (Figure 5).

For the piles with a conical shaped driving shoe the shaft grout showed a corkscrew shaped surface (Figure 6) which might be an explanation for the higher shaft resistances of piles PP2a, PP2b and PP6a compared to pile PP5a with the flat driving shoe.

For tension pile PP8a an abrupt failure was observed. The shaft grout was lifted approx. 5.5 cm from the top of the socket which indicate a structural failure of the prototype trilobular socket, which is still in its early development phase.

Figure 5. Pile PP4a after excavation

Figure 6. PP6a after excavation

5 CONCLUSIONS

The pile resistances achieved by means of conventional static load tests and the Pile H-P-S tests showed a good agreement.

The discrepancy between the results of the dynamic and the static tests, with the pile resistances derived from the dynamic tests being significantly higher than the resistances measured in the static tests, indicates the importance of a careful calibration of the dynamic tests as required for example in the EA-Pfähle (DGGT 2014), especially in cohesive soils.

The re-use of dynamically tested piles as foundation piles should not be considered as the impact caused by the free fall mass may impair the bond between ductile pipe and shaft grout.

The influence of the shape of the driving shoe on the base resistance, showing the potential of optimizing the bearing behaviour of the ductile piles, requires further investigation.

6 REFERENCES

Briaud, J.-L., Ballouz, M., Nasr, G. 2000. Static capacity prediction by dynamic methods for three bored piles. Journal of Geotechnical and Geoenvironmental Engineering, ASCE, New York, Vol. 126, No. 7, 640-649.

Deutsche Gesellschaft für Geotechnik (DGGT). 2014. Recommendations on Piling (EA-Pfähle). Verlag Wilhelm Ernst & Sohn, Berlin

Deutsches Institut für Bautechnik (DIBt) 2017. Allgmeine bauaufsichtliche Zulassung Z-34.25-230 TRM DUKTILPFAHL

Fleming, W.G.K., Weltman, A.J., Randolph, M.F., Elson, W.K. 2009. Piling Engineering. 3rd ed.; Taylor & Francis Group

Hayden, M. 2011. Pile HAY-Proof-System® (Pile H-P-S) - New Test Method for Static Load Tests of Slender Piles. Proc. 11th ISM Int. Workshop on Micropiles, Milan

Hayden, M., Kirchmaier, T. 2010. Pile HAY-Proof-System (Pile HPS) Neuartiges System für statische Probebelastungen an schlanken Pfählen. Veder-Kolloquium, Gruppe Geotechnik, TU Graz.

Klingmüller, O., Schallert, M. 2012. Resistance factors of high-strain dynamic testing regarding German application of Eurocode 7 and correlation of dynamic and static pile tests. Proceedings, 9th Int. Conf. on testing and Design Methodes for Deep Foundations, Kanazawa, Japan, 687 - 695

Svinkin, M.R. 2011. Engineering Aspects in Evaluation of Pile Capacity by Dynamic Testing. ASCE Structures Congress. Las Vegas, Nevada, USA, 1686 – 1697

Wehr, J., Andreas, M., Böhle, B., Schallert, M., Klingmüller, O. 2015. Real-time quality monitoring and result verification by static and dynamic trail loading of piles in marine clay. Proceedings, 16th European Conf. on Soil Mechanics and Geotechnical Engineering. Edinburgh, Scotland, 1339 - 1343